Nanopipe fabrication using vertically aligned carbon nanofiber templates

A. V. Melechko[a)]
Molecular-Scale Engineering and Nanoscale Technologies Research Group, Oak Ridge National Laboratory, Oak Ridge, Tennessee 37831 and University of Tennessee Center for Environmental Biotechnology, Knoxville, Tennessee 37996

T. E. McKnight
Molecular-Scale Engineering and Nanoscale Technologies Research Group, Oak Ridge National Laboratory, Oak Ridge, Tennessee 37831

M. A. Guillorn and D. W. Austin
Molecular-Scale Engineering and Nanoscale Technologies Research Group, Oak Ridge National Laboratory, Oak Ridge, Tennessee 37831 and University of Tennessee Material Science and Engineering Department, Knoxville, Tennessee 37996

B. Ilic
Cornell University, Ithaca, New York 14853

V. I. Merkulov
Molecular-Scale Engineering and Nanoscale Technologies Research Group, Oak Ridge National Laboratory, Oak Ridge, Tennessee 37831

M. J. Doktycz
Life Science Division, Oak Ridge National Laboratory, Oak Ridge, Tennessee 37831

D. H. Lowndes
Thin Film and Nanostructure Physics Group, Oak Ridge National Laboratory, Oak Ridge, Tennessee 37831

M. L. Simpson
Molecular-Scale Engineering and Nanoscale Technologies Research Group, Oak Ridge National Laboratory, Oak Ridge, Tennessee 37831; University of Tennessee Center for Environmental Biotechnology, Knoxville, Tennessee 37996; and University of Tennessee Material Science and Engineering Department, Knoxville, Tennessee 37996

We report a method to fabricate tubular nanostructures using vertically aligned carbon nanofibers grown by plasma-enhanced chemical vapor deposition as templates. The resulting nanopipes are oriented perpendicular to the substrate and have internal diameters ranging from 30 to 200 nm and can be up to several micrometers in length. These nanopipes can be deterministically positioned on a substrate and arranged into singular devices or arrays. *© 2002 American Vacuum Society.* [DOI: 10.1116/1.1515306]

I. INTRODUCTION

Approaches to fabrication are needed for devices that require functional nanoscale features within a microscale or larger structure. A well-known approach provides structure to device components through a patterned sacrificial material layer.[1,2] A progression of this approach is the use of materials that self-assemble into nanostructures, such as carbon nanotubes (CNTs) and carbon nanofibers (CNFs), as sacrificial templates. These templates can bestow properties of size, orientation, or placement on materials that would not otherwise assemble into such configurations. This hierarchical approach to nanofabrication allows the extension of self-assembly properties to many materials and provides a viable way to simultaneously engineer devices over size scales that vary by many orders of magnitude.

In this article we demonstrate the use of carbon nanofibers as sacrificial templates for nanopipes, which are extended structures that can be as long as a few micrometers with internal diameters ranging from 200 nm down to 30 nm. Such nanopipes can be implemented as functional elements in gas- and liquid-phase fluidic, biomimetic, and sensing devices. Several applications of such devices can be envisioned including high-throughput sensing and analysis of molecular species, control elements in active fluidic transport systems, fluidic interfaces to viable cells or cell communities (e.g., biofilms), and as nanoporous membranes[2,3] for molecular transport manipulation with very good control of the nanopore geometry.

The utility of vertically aligned carbon nanofibers (VACNFs) for nanoscale devices has been established, as a variety of nanodevices utilizing VACNFs have been fabricated. These include electrochemical probes designed for intracellular characterization,[4] gated cathode field emitters,[5,6] and biomimetic membrane structures.[7] VACNFs that are a few tens of nanometers in diameter and up to several microns long can be catalytically grown by plasma-enhanced chemical vapor deposition (PECVD).[8–11] The position of each nanofiber can be defined by a patterning catalyst using
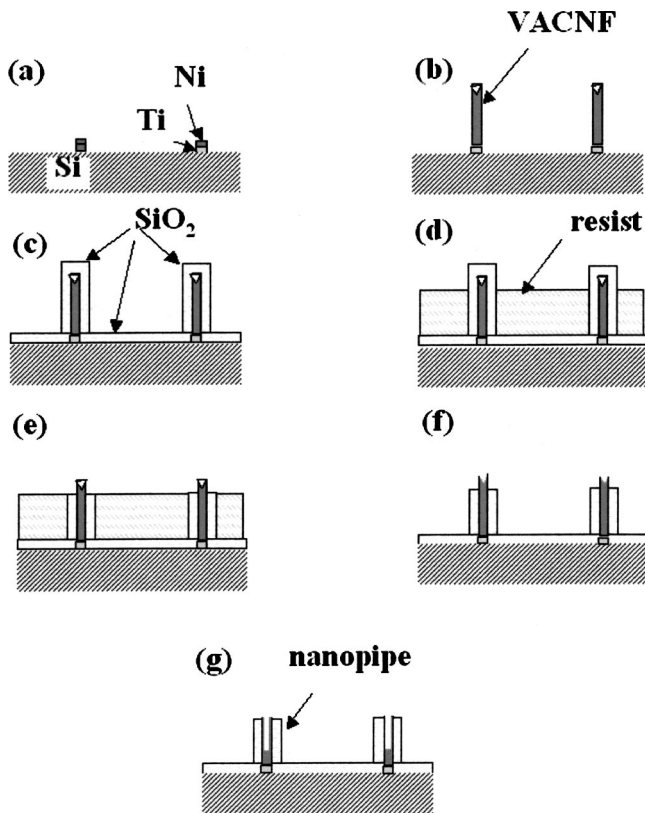

FIG. 1. Steps for fabrication of isolated nanopipes: (a) Ni particles are defined via EBL and the lift-off technique; (b) VACNF grown by PECVD; (c) VACNFs and substrate are coated with SiO_2 by PECVD; (d) resist is spun on and the VACNF tips are opened; (e) SiO_2 is removed from the tips by RIE; (f) Ni particle is removed in HNO_3 wet etch; and (g) VACNF is etched away in O_2 plasma.
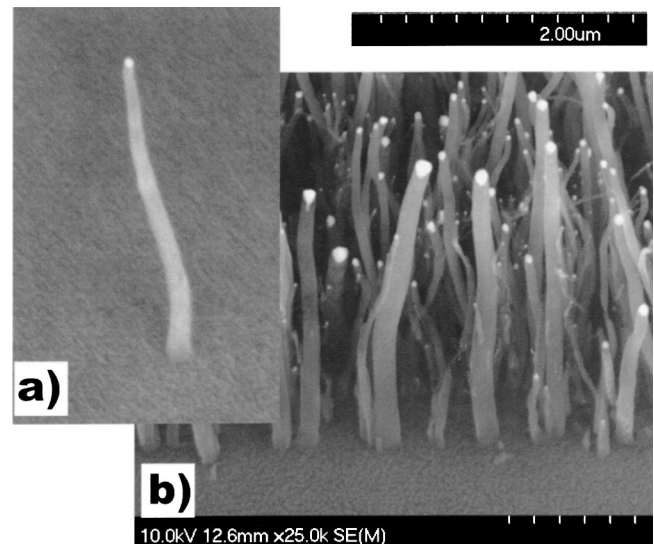

FIG. 2. SEM images of an isolated and a dense forest of VACNF grown from unpatterned catalyst (viewed at 30°). The bright spots are Ni particles.

photo- or electron-beam lithography (EBL) or potentially by methods that self-assemble arrays of nanodots (for example, see Ref. 12), and their orientation is determined by the direction of the electric field lines during the growth process.[9,10]

Here we show that these properties of VACNF growth can be transferred to the controlled synthesis of nanopipes that can be deterministically created with defined location, number (e.g., array or single), length, and internal diameter. The fabrication of nanopipes as described here can be integrated in a parallel manner into microstructured substrates and lab-on-a-chip devices as we have previously demonstrated with VACNF-based devices.[4,6,7] This process can be extended further with the use of nanopipes as secondary templates. We demonstrate this with the fabrication of metallic nanowires.

II. FABRICATION

The nanopipe fabrication process is depicted in Fig. 1. The VACNF catalyst particles were deposited on a Si substrate using a lift off process [Fig. 1(a)]. Electron-beam resist, poly(methylmethocrylate) (PMMA), was spun on the top surface and patterns were exposed. The size of the exposed dots was chosen to be 100 nm in diameter to produce isolated VACNFs.[8] The exposures were developed in a solu-

tion of MIBK: isopropanol 1:1 for 1 min, rinsed in isopropanol and blown dry with nitrogen. The Ti buffer layer (10 nm) and catalyst metal (Ni, 10 nm) were deposited by electron gun physical vapor deposition (PVD). The resist was then dissolved in acetone so that the metal remained only on the exposed areas. The VACNFs were grown [Fig. 1(b)] in a glow discharge dc plasma of ammonia/acetylene (80 sccm/40 sccm) gas mixture at 700 °C, with 2.5 Torr total pressure and 150 mA dc current. Carbonaceous species decompose at the surface of the Ni particle, free carbon diffuses through this particle, and it is deposited on the bottom surface of the catalyst as described previously.[13] Since the synthesis is catalytically controlled, a VACNF emerges only at the positions where the catalyst was placed. The resultant isolated VACNF and a dense forest of VACNFs grown from unpatterned catalyst are shown in Fig. 2.

In the next step [Fig. 1(c)] the nanofibers and the surface of the chip were coated with a 100-nm-thick layer of SiO_2 using a silane-based PECVD process to form the walls of the nanopipes. The scanning electron microscopy (SEM) images of encapsulated nanofibers are shown in Figs. 3(a) and 3(b). To open the tips of the nanopipes, resist was spun over the surface of the chip (Shipley, Microposit 1818) and its thickness was adjusted by reactive ion etching (RIE) in oxygen plasma to uncover the tips of the nanopipe structures [Fig. 1(d)]. The silicon oxide was removed from exposed areas using RIE in CHF_3/O_2 rf plasma [Fig. 1(e)]. The resist was then dissolved in acetone or, alternatively, etched in RIE oxygen-based plasma. The latter method is preferable since it uncovered the catalyst particle from the carbon film that covered it after VACNF growth.[14] A small amount of the top portion of the carbon nanofiber was etched directly under the catalytic particle [Fig. 3(c)] during this RIE step, but VACNF etching did not continue with increased etch time. Thus this step was followed by a 1 min dip in nitric acid to remove the
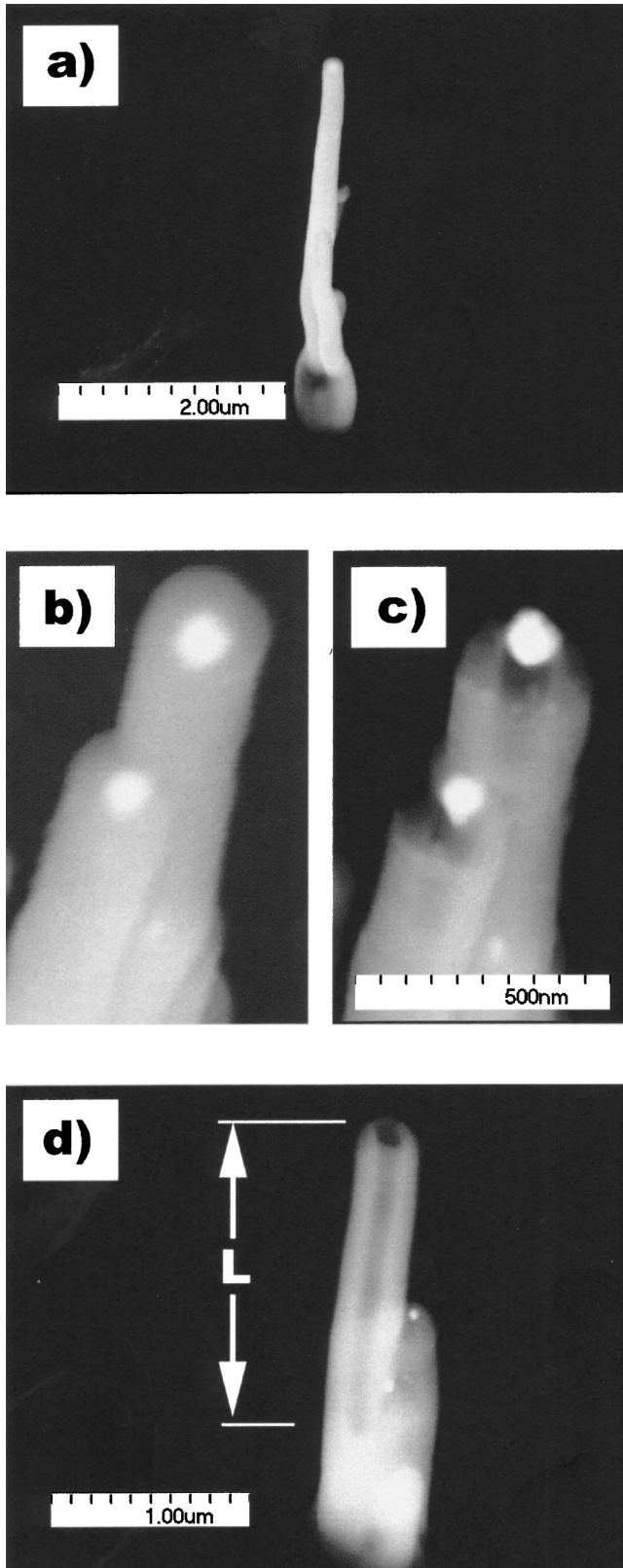
FIG. 4. Depth of the nanopipes vs etching time.

FIG. 3. SEM images of nanopipes at various steps during the fabrication process: (a) an isolated VACNF encased in SiO_2 (80 nm); (b) an enlarged view of two VACNFs coated with SiO_2 with a Ni nanoparticle visible as a bright spot; (c) encapsulation is opened at the tips and part of the VACNF is removed (slightly darker area along the VACNF axis); and (d) the VACNF is partially etched out from inside the nanopipe.
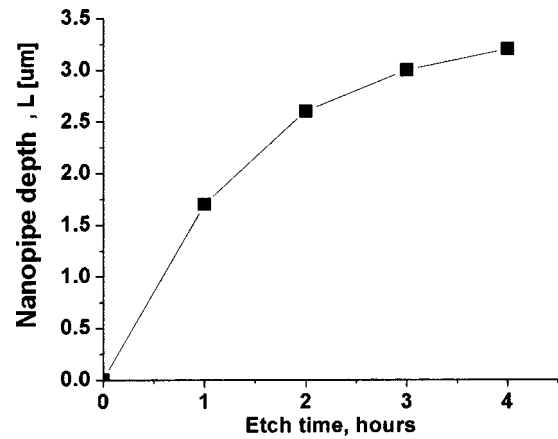
Ni particle that blocked access of etchant species (oxygen radicals) to the body of the VACNF [Fig. 1(f)].

With this access to the VACNF provided, subsequent RIE in an oxygen plasma produced nanopipes [Figs. 1(g) and 3(d)]. The etching rate depended on the diameter of the nanofiber since a smaller diameter nanopipe was more restrictive to diffusive access of etchant species. Likewise, the etching rate strongly decreased with time due to increased nanopipes depth (Fig. 4). This effect ultimately limits the length of the possible nanopipe structures made using reactive ion etching. Other methods of carbon oxidation and removal may provide the means to produce higher aspect ratio nanopipes.

III. FUNCTIONALITY

To characterize the quality of the internal structure of the nanopipes and to test functionality as electrochemical nanoprobes (fluidic and ion transport properties) we performed metal electrodeposition experiments. For these experiments we reduced Au from electroplating solution (Orotherm HT, Technic, Inc) inside the nanopipes to form Au nanowires. A Pt wire dipped into solution above the structures served as the anode, and the remains of the carbon nanofibers at the bottom of the nanopipes where the cathodes contacted in parallel through the Si substrate. In order to remove air bubbles from the nanopipes, the sample was soaked and refrigerated in electroplating solution for 1 h. 1 μm long nanowires (bright rods in Fig. 5) were formed after plating for 1 h at $60\,°C$ with -1 V on the cathode and current compliance of the reducing voltage power supply set to 1 μA. The large cluster of gold in Fig. 5 was formed quickly after one of the nanopipes was completely filled and mass transport to the electroactive surface was less restricted. The limited access of gas or liquid to the interior of the nanopipes may be used to our advantage. For example, the rate of the metal electrodeposition inside the nanopipe is much smaller than that at open tip nanostructures, and consequently can be more precisely controlled. We have observed that the rate of gold electroplating inside the nanopipes (Fig. 5) is at least two orders of magnitude slower than the rate at the exposed
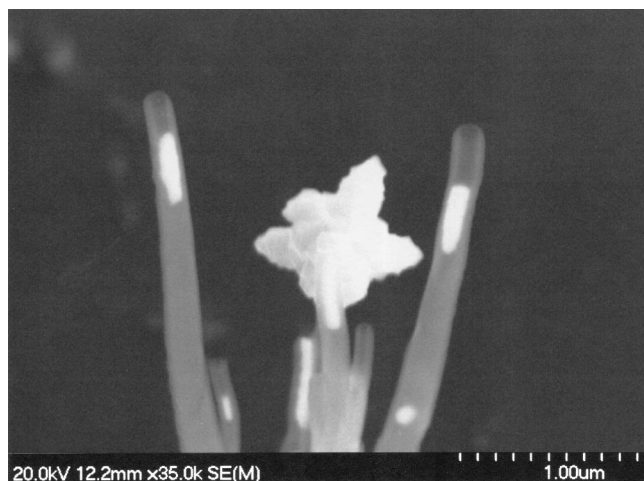
FIG. 5. SEM image of the nanopipes with gold electroplated inside (viewing angle is 30°). The large gold cluster in the center is above a completely filled nanopipe.

tip of the nanofiber electrochemical probe.[4] Thus varying electrodeposition duration can precisely control nanostructure formation within nanopipes.

Structures produced by metal electroplating within nanopipe templates may be used in several applications. The Au plating on probes may be used to exploit thiol chemistry in biosensing, electroplating of Ni or Fe may be useful to produce nanorods for magnetic applications (e.g., magnetic force microscopy tips, etc.), and nanowires of many types may find uses in electronics. The main advantage of this approach, compared, for example, to the use of porous membranes,[2] is that the nanowires can be produced at any desired location due to the deterministic growth characteristics of VACNFs.

IV. CONCLUSIONS

A method of nanofabrication based on the synthesis of sacrificial self-assembled nanostructures (VACNFs) as templates for nanopipes has been demonstrated. The carbon nanofibers are grown from catalytically defined points on a substrate, conformally coated with structural material such as SiO_2, and etched away in oxygen plasma after access holes are opened. The use of nanopipes as secondary templates for making metal nanowires by electrodeposition has been also demonstrated.

[1]C. K. Harnett, G. W. Coates, and H. G. Craighead, J. Vac. Sci. Technol. B **19**, 2842 (2001).

[2]C. R. Martin, Science **266**, 1961 (1994).

[3]J. Li, D. Stein, C. McMullan, D. Branton, M. J. Aziz, and J. A. Golovchenko, Nature (London) **412**, 166 (2001).

[4]M. A. Guillorn, T. E. McKnight, A. Melechko, V. I. Merkulov, P. F. Britt, D. W. Austin, D. H. Lowndes, and M. L. Simpson, J. Appl. Phys. **91**, 3824 (2002).

[5]L. R. Baylor, V. I. Merkulov, E. D. Ellis, M. A. Guillorn, D. H. Lowndes, A. V. Melechko, M. L. Simpson, and J. H. Whealton, J. Appl. Phys. **91**, 4602 (2002).

[6]M. A. Guillorn, A. V. Melechko, V. I. Merkulov, E. D. Ellis, C. L. Britton, M. L. Simpson, D. H. Lowndes, and L. R. Baylor, Appl. Phys. Lett. **79**, 3506 (2001).

[7]L. Zhang, A. V. Melechko, V. I. Merkulov, M. A. Guillorn, M. L. Simpson, D. H. Lowndes, and M. J. Doktycz, Appl. Phys. Lett. **81**, 135 (2002).

[8]V. I. Merkulov, D. H. Lowndes, Y. Y. Wei, G. Eres, and E. Voelkl, Appl. Phys. Lett. **76**, 3555 (2000).

[9]V. I. Merkulov, A. V. Melechko, M. A. Guillorn, D. H. Lowndes, and M. L. Simpson, Appl. Phys. Lett. **79**, 2970 (2001).

[10]V. I. Merkulov, A. V. Melechko, M. A. Guillorn, M. L. Simpson, D. H. Lowndes, J. H. Whealton, and R. J. Raridon, Appl. Phys. Lett. **80**, 4816 (2002).

[11]Z. F. Ren, Z. P. Huang, J. W. Xu, J. H. Wang, P. Bush, M. P. Siegal, and P. N. Provencio, Science **282**, 1105 (1998).

[12]S. W. Lee, C. B. Mao, C. E. Flynn, and A. M. Belcher, Science **296**, 892 (2002).

[13]R. T. K. Baker, Carbon **27**, 315 (1989).

[14]A. V. Melechko, V. I. Merkulov, D. H. Lowndes, M. A. Guillorn, and M. L. Simpson, Chem. Phys. Lett. **356**, 527 (2002).